Surface Science 602 (2008) 2264–2270

Contents lists available at ScienceDirect

Surface Science

journal homepage: www.elsevier.com/locate/susc

The structure and reactivity of 2-butanol on Pd(1 1 1)

Feng Gao [a], Yilin Wang [a], Luke Burkholder [a], Carol Hirschmugl [b], Dilano K. Saldin [b], Hin Cheuk Poon [b], David Sholl [c], Joanna James [d], Wilfred T. Tysoe [a,*]

[a] Department of Chemistry and Biochemistry and Laboratory for Surface Studies, University of Wisconsin-Milwaukee, Milwaukee, WI 53211, USA
[b] Department of Physics and Laboratory for Surface Studies, University of Wisconsin-Milwaukee, Milwaukee, WI 53211, USA
[c] School of Chemical and Biomolecular Engineering, Georgia Institute of Technology, Atlanta, GA 30332, USA
[d] Department of Chemical Engineering, Carnegie-Mellon University, Pittsburgh, PA 12345, USA

ARTICLE INFO

Article history:
Received 31 March 2008
Accepted for publication 6 May 2008
Available online 16 May 2008

Keywords:
2-Butanol
Pd(1 1 1)
Temperature-programmed desorption
Low-energy electron diffraction
Density functional theory

ABSTRACT

The structure, formation and decomposition pathways of 2-butoxide species formed on a Pd(1 1 1) surface following the adsorption of 2-butanol is studied by a combination of density functional theory (DFT), analysis of the low-energy electron intensity versus beam energy curves (LEED I/E) and temperature-programmed desorption (TPD). Both DFT calculations and LEED I/E measurements reveal that 2-butoxide adsorbs with the oxygen atom located in the three-fold hollow sites on Pd(1 1 1) with the C–O bond almost perpendicular to the surface with the 2-butyl group in the trans configuration. At coverages below ~0.11 monolayers, adsorbed 2-butoxide species completely thermally decompose to desorb hydrogen and carbon monoxide. The 2-butoxide species present at higher coverages either hydrogenate to reform 2-butanol or undergo a β-hydride elimination reaction to form 2-butanone.

1. Introduction

Pd(1 1 1) surfaces modified by adsorbed chiral 2-butanol have been shown to lead to the enantioselective chemisorption of propylene oxide. That is, pre-covering a Pd(1 1 1) surface with either *R*- or *S*-2-butanol leads to a preferential adsorption of propylene oxide of the same chirality over a narrow 2-butanol coverage range [1,2]. This effect was initially ascribed to enantioselectivity induced by chiral 2-butoxide species formed by dehydrogenation of 2-butanol [1]. However, it was found more recently that this effect was in fact due to enantiospecific hydrogen-bonding interactions between 2-butanol and propylene oxide [2]. Measurements of the variation in enantiospecificity with 2-butanol exposure suggested that propylene oxide can interact either with a single adsorbed 2-butanol molecule or, at higher coverages, with two adsorbed 2-butanol species to form enantioselective sites [3]. More recently, 2-butanol has been used as a chiral probe for enantioselectivity on surfaces modified by an amino acid [4].

Although the formation of 2-butoxide is not directly relevant to enantioselective chemisorption described above, it is nevertheless important to understand surface chemistry of 2-butanol (and other C_4+ alcohols), which have received much less attention in the past than smaller alcohols [5,6]. Reflection–absorption infrared spectroscopy (RAIRS) revealed that the adsorbed 2-butanol dehydrogenated to form 2-butoxide, which underwent a β-hydride elimination reaction to yield 2-butanone [1]. The work described below focuses on the surface chemistry of 2-butanol in greater detail using temperature-programmed desorption (TPD) and by determining the structure of the 2-butoxide intermediate using low-energy electron diffraction (LEED) measurements. Compared with X-ray diffraction structure measurements, which may be modeled by single-scattering theory, "direct methods" for electron diffraction, a strong multiple-scattering problem, are still very much under development [7]. It is thus customary in determining surface structures using LEED to calculate experimental intensity *versus* beam energy (I/E) curves for all likely adsorbate structures and compare these with the experimental data to establish the correct structure [8]. While this approach is feasible for adsorbates with a relatively small number of degrees of freedom, it rapidly becomes prohibitive for larger molecules such as 2-butanol. In order to address this problem, the 2-butoxide structure on a Pd(1 1 1) surface is calculated using density functional theory (DFT). This provided a limited number of structures, which can then be compared with the experimental I/E curves to provide the correct surface structure.

2. Experimental methods

Temperature-programmed desorption (TPD) data were collected in an ultrahigh vacuum chamber that has been described

* Corresponding author. Tel.: +1 414 229 5222; fax: +1 414 229 5036.
E-mail address: wtt@uwm.edu (W.T. Tysoe).

0039-6028/$ - see front matter © 2008 Elsevier B.V. All rights reserved.
doi:10.1016/j.susc.2008.05.008

in detail elsewhere [9] where desorbing species were detected using a Dycor quadrupole mass spectrometer placed in line of sight of the sample. The temperature ramp and data collection were controlled using LabView software. All TPD spectra were recorded using a heating rate of 6.5 K/s in this study.

LEED I/E curves were measured in a low current system with an incident beam current of ~500 fA using a system described previously [10]. The diffracted beam was amplified using a microchannel plate and the position of the amplified electron pulse determined using a wire grid system. This allowed a full I/E curve to be obtained for less than one electron interacting with each adsorbate molecule.

The Pd(1 1 1) sample was cleaned using a standard procedure which consisted of heating at 1000 K in $\sim 4 \times 10^{-8}$ Torr of oxygen and then annealing at 1200 K *in vacuo* to remove any remaining oxygen. Since a strong palladium peak effectively obscures the carbon KLL Auger feature, Auger spectroscopy is insensitive to the presence of small amounts of surface carbon. A sensitive gauge of carbon coverage was to saturate the surface with oxygen and to perform a temperature-programmed desorption experiment. The presence of surface carbon is manifest by the desorption of CO. As the surface becomes depleted of carbon, the CO yield decreases and the yield of oxygen increases correspondingly. The complete absence of carbon is indicated by the desorption of only O_2.

2-butanol (Aldrich, 99.5%) was transferred to glass bottles and attached to the gas-handling systems of the vacuum chambers and was further purified by several freeze-pump-thaw cycles. The cleanliness of all reactants was monitored mass spectroscopically.

3. Theoretical methods

The I/E curves from the 2-butoxide-covered sample were simulated for normal incidence by assuming an ordered overlayer of the smallest possible (1×1) periodicity with fractional occupancy of the same magnitude as the coverage Θ. This idea that the intensities of integer-order beams may be calculated by considering their interactions with just other integer-order beams may be regarded as a special case of the beam set neglect method [11,12]. The additional simplification is that the quasidynamical [13] treatment of the adlayer allows it to be treated as literally a (1×1) overlayer with an adsorbate scattering factor reduced by a factor of Θ, so that the coverage appears as a variable in the LEED structure determination [14–18].

Plane wave density functional theory calculations were performed using the Vienna *ab initio* Simulation Package (VASP) and the ultrasoft pseudopotentials available in this package [19]. VASP has been shown to give results that are in agreement with other DFT packages [20,21]. The results reported here are from calculations with the generalized gradient approximation (GGA) using the Perdew–Wang 91 functional [22]. We used a $3 \times 3 \times 1$ Monkhorst–Pack [23] *k*-point sampling of the Brillouin zone and a plane wave expansion with a cutoff of 396 eV. To examine the structure of isolated 2-butoxide on Pd(1 1 1), all calculations placed a single adsorbed molecule in a (3×3) surface unit cell. The Pd (1 1 1) surface was represented by a slab four layers thick with a vacuum spacing of 14 Å. The top two layers of the slab were allowed to relax with the adsorbed molecule, since the adsorbate is expected to exhibit some effect on the substrate. The DFT-optimized lattice constant for Pd was used to define the surface. This lattice constant, 3.96 Å, is in good agreement with the experimental value of 3.89 Å [24]. All calculations involved convergence of relaxed atomic forces to within 0.03 eV/Å and include dipole corrections [22,25] in the direction normal to the surface.

4. Results

4.1. Surface Structure Determination

We have shown previously that the structure of disordered overlayers can be determined from the change in the I/E curves of the substrate (1×1) Bragg spots due to the presence of the overlayer [14–18]. In this case, the overlayer structure is determined by simulating an ordered overlayer of the smallest possible (1×1) periodicity with fractional occupancy of the same magnitude as the coverage Θ. This approach has been successful in establishing the structures of a number of surface species. Comparison of the structures measured by LEED with those calculated by DFT yielded excellent agreement in all cases. Since it is a prohibitively large task to compare the calculated structures of all possible configurations of relatively large adsorbates such as 2-butoxide species, our approach is to compare the structure of 2-butoxide calculated using DFT with the experimental LEED I/E curves to establish whether the calculated structure is indeed correct.

To examine the structure of isolated 2-butoxide on Pd(1 1 1), we initially placed a single adsorbed molecule in a (3×3) surface unit cell with the O–C bond centered over fcc, hcp, atop and bridge sites. DFT calculations showed that the 2-butoxide adsorbs on the surface with the oxygen atom located above the Pd(1 1 1) three-fold hollow site with the O–C bond oriented approximately perpendicular to the surface. Other stable sites included those near the hcp, atop and bridge sites, but were less stable by 0.19 eV to 0.36 eV. To ensure that these molecules were isolated and that there were no interactive effects in this study, we also placed a single adsorbed molecule in a (4×3) surface unit cell with the butyl group oriented along the length of the unit cell. These calculations showed an identical bonding preference. The 2-butyl group is in the trans configuration with its plane oriented approximately parallel to the surface. This surface structure is shown graphically in Fig. 1 for a surface coverage of 1/9 ($\Theta = 0.11$) and the interatomic distances and angles are given in Table 1. We also examined the azimuthal rotational energy barrier using DFT by rotating the molecule by 10° increments through 120°. Our calculations indicate that the energy barrier to azimuthal rotation is only 0.05 eV,

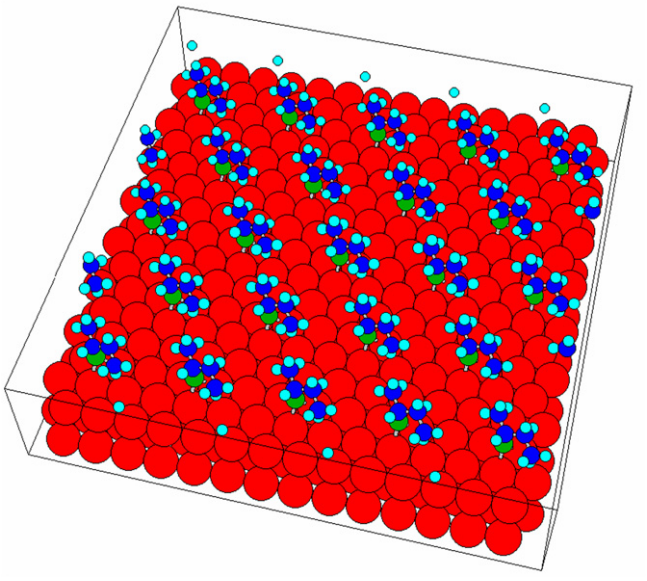

Fig. 1. Schematic depiction of the structure of 2-butoxide species on a Pd(1 1 1) surface with a coverage of 0.11.

Table 1
The structural properties of 2-butoxide on Pd(1 1 1) calculated using density functional theory

	2-Butoxide/Pd(1 1 1) from DFT
d(O–C)/Å	1.45
d(C–C)/Å	1.52, 1.53, 1.52
d(C–H)/Å	1.10
d(O–Pd)/Å	2.16, 2.18, 2.21
θ(O–C–C)/°	109, 110
θ(C–O angle to surface normal)/°	8

suggesting that adsorbed molecules can rotate relatively freely, at least at low coverages.

Initial experiments were carried out to search for ordered LEED patterns. While none were found at intermediate exposures, a very weak $\sqrt{3} \times \sqrt{3}R30°$ LEED pattern was detected at 2-butoxide coverages close to saturation (following a 2-butanol exposure of ~1.6 L, see below). This implies that the saturation 2-butoxide coverage should be less than 0.33 (where coverages are referenced to the palladium atom density on the (1 1 1) surface). The LEED I/E curves were collected at normal incidence for all spots visible on the LEED screen for a surface exposed to 1.6 L of 2-butanol and then heated to 200 K to form the 2-butoxide species. This exposure was selected to avoid the possibility of adsorption of contaminants from the background. There is therefore a possibility of inducing a rotation of the methyl group around the C_2–C_3 axis due to crowding of the adsorbed 2-butoxide species. Thus, the Pendry R-factor [26] was calculated for the structure determined from DFT (Fig. 1 and Table 1) for various coverages (Θ(2-butoxide) = 0.5, 0.3 and 0.25) as a function of rotation around the C_2–C_3 axis. The results are displayed in Fig. 2 where the Pendry R-factor is plotted versus C_2–C_3 rotation angle for Θ(2-butoxide) = 0.5 (▲), 0.3 (●) and 0.25 (■). The results show a considerable variation in the R-factor with C_2–C_3 rotation angle with the lowest values being found for an angle between ~250 and 300°. The value calculated from DFT is indicated by the vertical line on Fig. 2 and is in good agreement with the value obtained from the LEED analysis. The curves also depend on the coverage used for the LEED calculations with consistently lower values being obtained for Θ(2-butoxide) = 0.25, although the curve for Θ(2-butoxide) = 0.3 is not substantially worse. These results indicate that the 2-butoxide structure determined by DFT calculations is in excellent agreement with that from LEED I/E curves and that the saturation 2-butoxide coverage is ~0.25–0.3, consistent with the observation of a faint $\sqrt{3} \times \sqrt{3}R30°$ LEED pattern.

4.2. Temperature-programmed desorption

Fig. 3 displays a series of 74 amu (2-butanol) TPD spectra collected as a function of 2-butanol exposure, where 2-butanol was adsorbed on the surface at ~100 K and the heating rate was set at 6.5 K/s. At 2-butanol exposures of 0.4 L and below, no molecular desorption was detected, indicating complete 2-butanol decomposition. However, for exposures of 0.6 L and higher, desorption is detected at ~285 K with a desorption temperature that decreases with increasing exposures so that at an exposure of 1.8 L, corresponding to a saturated overlayer, 2-butanol desorbs at ~235 K. An additional sharp feature appearing at ~140 K for the highest 2-butanol exposure is due to adsorption in the second layer.

Ketone formation was detected previously by RAIRS [1]. There are no intense mass spectrometer ionizer fragments that are diagnostic for 2-butanone that do not also occur for 2-butanol. However, the 72 amu signal is selected to monitor 2-butanone since the I(72 amu)/I(74 amu) for 2-butanol is ~3.0 with the mass spectrometer used for this work so that 2-butanol contributions to the 72 amu spectrum can easily be subtracted. The 72 amu spectra are plotted in Fig. 4a as a function of 2-butanol exposure, where expo-

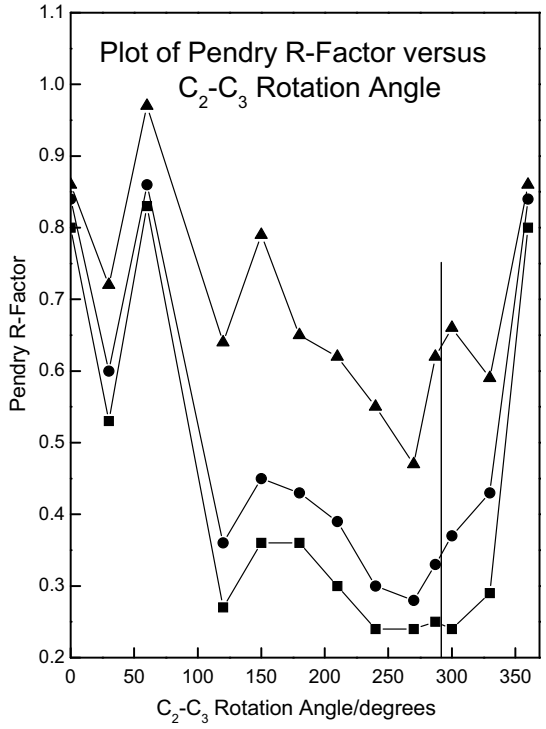

Fig. 2. Plot of the Pendry R-factor versus the angle of rotation about the C_2–C_3 bond of 2-butoxide species adsorbed on a Pd(1 1 1) surface using the results of density functional theory calculations as input into the LEED analysis program, for Θ(2-butoxide) = 0.25 (■), 0.3 (●) and 0.5 (▲).

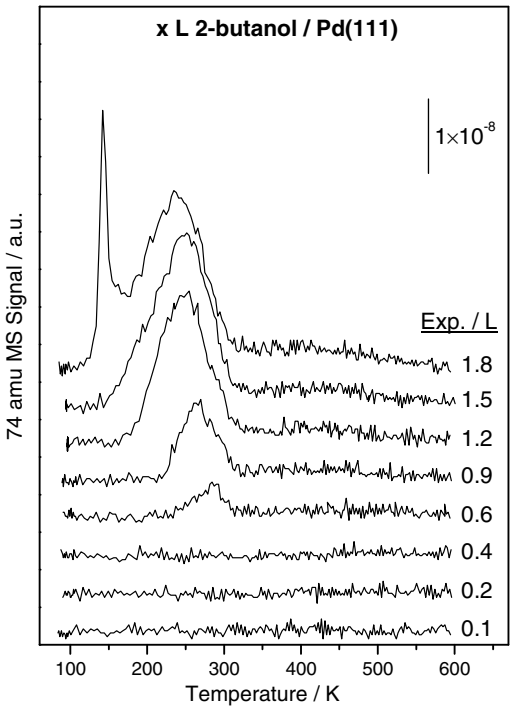

Fig. 3. Temperature-programmed desorption data monitoring 74 amu (2-butanol) following adsorption of 2-butanol on clean Pd(1 1 1) at 80 K at a heating rate of 6.5 K/s as a function of 2-butanol exposure, where exposures are marked adjacent to the corresponding spectrum.

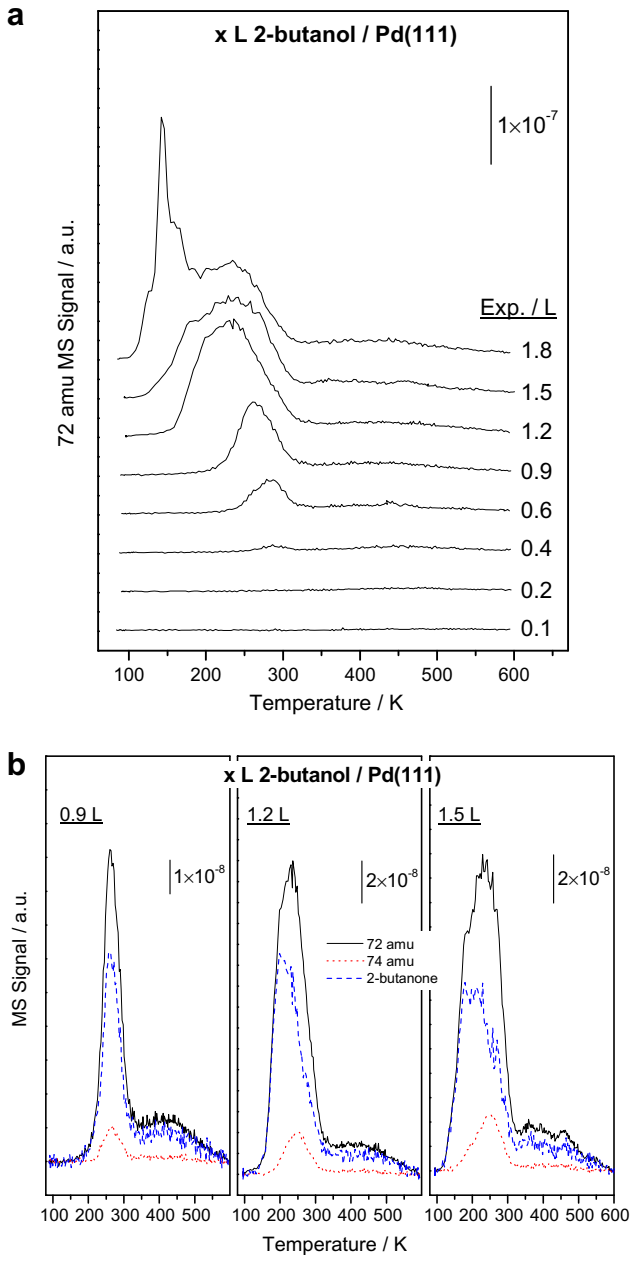

Fig. 4. Spectra (a): TPD spectra monitoring 72 amu (predominantly 2-butanone) collected following adsorption of 2-butanol on clean Pd(1 1 1) at 80 K at a heating rate of 6.5 K/s as a function of 2-butanol exposure, where exposures are marked adjacent to the corresponding spectrum. The spectra displayed in (b) show the desorption profiles due to 2-butanaone alone after the contribution due to 2-butanol fragmentation has been removed.

sures are marked adjacent to the corresponding spectrum. At a 2-butanol exposure of 0.4 L, where no molecular 2-butanol desorption was found (Fig. 3), a weak 72 amu signal is detected at ~290 K and is assigned to 2-butanone desorption. At higher 2-butanol exposures, the 72 amu signals are much wider than the 74 amu signals (Fig. 3) suggesting that these are not due predominantly due to 2-butanol desorption and include fragments due to both 2-butanol and 2-butanone. It is straightforward to perform a simple deconvolution to obtain the 2-butanone desorption profiles by subtracting the 2-butanol contribution to the 72 amu signals, and the results are plotted in Fig. 4b. This reveals that the 2-butanone desorption temperature decreases with increasing 2-butanol exposure, indicating that this is a desorption-limited process. Second, at a 2-butanol exposure of 1.5 L, the 2-butanone yield decreases slightly compared with that found at an exposure of 1.2 L. This can be understood by the proposing that β-hydride elimination is hindered to some extent by a crowded surface. Finally, it should be pointed out that 2-butanol has only a very weak 74 amu fragment (only 0.5% of the strongest signal at 45 amu) while 2-butanone has a strong signal at 72 amu (25% of the strongest signal at 43 amu). Assuming the relative sensitivity ratios of 45 amu signal for 2-butanol and 43 amu signal for 2-butanone are in the same order of magnitude, it is estimated that only a few percent of adsorbed 2-butanol coverts to 2-butanone.

As shown in Fig. 3, no molecular desorption was found at 2-butanol exposures of 0.4 L and lower and the data in Fig. 4 reveal that only limited amount of 2-butanone is generated. Therefore other masses were monitored to search for other gaseous products. Fig. 5a displays a number of masses at a 2-butanol exposure of 0.9 L (prior to monolayer saturation). Note that these are collected in several TPD runs so that slight line-shape and temperature variations cannot be avoided. Nevertheless, the signal intensities correspond rather well with the fragmentation of 2-butanol suggesting that the formation of hydrocarbons and oxygenates (except 2-butanone), if any, is below the detection limit. This argument is further corroborated by performing a similar deconvolution to that displayed in Fig. 4b with other masses, and no detectable desorption of other gaseous products is revealed. Fig. 5b displays corresponding TPD spectra at a 2-butanol exposure of 1.8 L (after monolayer saturation). Again, there is no indication of the formation of other gaseous products. The 44 amu profile is also plotted in this graph, which contains some contribution from background CO_2 at low temperatures. It is worth pointing out that very weak methane desorption was found between 300 and 400 K (data not shown). Although weak, this desorbs at higher temperatures than 2-butanol so that can still be easily resolved.

The 2-butanol yield (obtained by integrating the desorption profiles in Fig. 1) is plotted in Fig. 6 as a function of exposure. At 2-butanol exposures of 0.9 L and greater, the 2-butanol yield increases almost linearly with exposure, suggesting a constant sticking probability at all exposures. The line intersects with the *x*-axis at ~0.68 L. This suggests that for exposures greater than 0.68 L, even though 2-butanol can still adsorb on the surface (monolayer saturation occurs at ~1.5 L), this additional 2-butanol does not dissociate and also implies that ~45% of the saturated 2-butanol overlayer dissociates.

Previous RAIRS investigations suggest that 2-butanol first deprotonates to form surface 2-butoxide species [1], which decomposes by a β-hydride elimination reaction to form 2-butanone. The above TPD results reveal the formation of a limited amount of 2-butanone and methane (data not shown) and no other hydrocarbons or oxygenates. This suggests that a portion of adsorbed 2-butoxide species undergo complete decomposition.

In order to explore this, 2 amu (H_2) desorption spectra were collected and the results are displayed in Fig. 7a as a function of 2-butanol exposure, where exposures are marked adjacent to the corresponding spectrum. At the lowest exposure (0.1 L), a single hydrogen desorption state is found centered at ~370 K. At higher exposures, in addition to this desorption state, another less intense state develops at ~480 K. Fig. 5b plots the integrated H_2 desorption peak yield as a function of exposure. This reveals that the H_2 yield saturates following an exposure of 0.6 L. Note that this corresponds rather well with the data presented in Fig. 4 indicting that no 2-butanol desorbs at exposure lower than ~0.68.

Fig. 8a presents the corresponding CO (28 amu) desorption data. Several desorption states are apparent. Desorption below 300 K can be assigned to background CO adsorption for 2-butanol exposures below 0.4 L, and fragmentation of 2-butanol, as well as

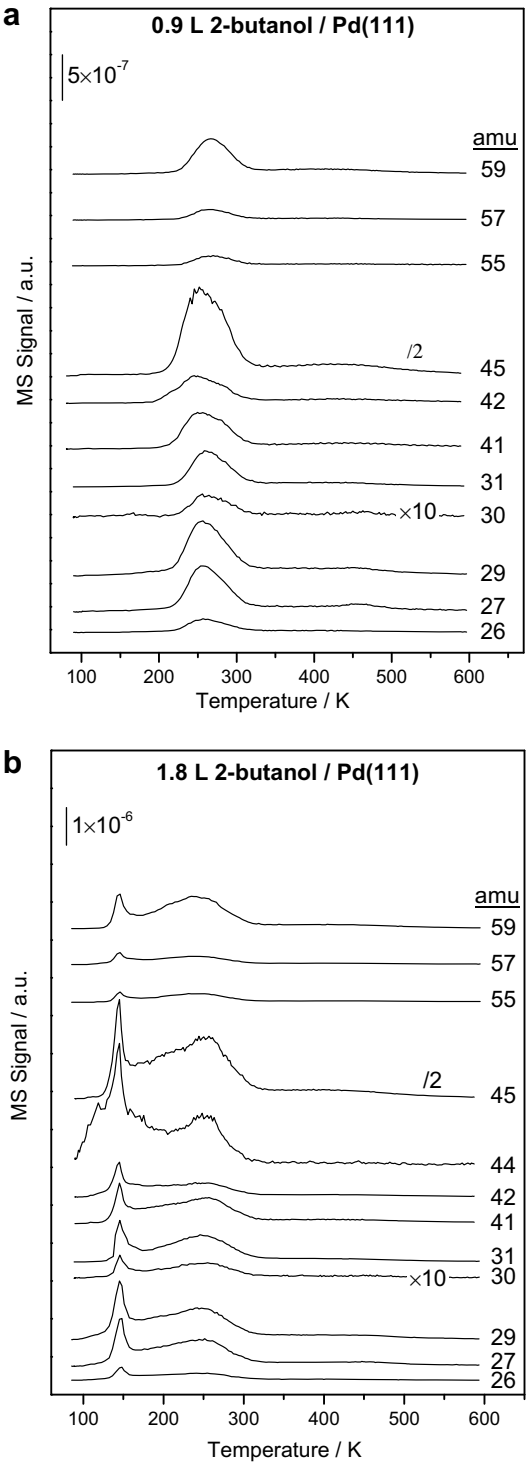

Fig. 5. TPD spectra collected at various masses following adsorption of 2-butanol on clean Pd(1 1 1) at 80 K at a heating rate of 6.5 K/s where the detected masses are marked adjacent to the corresponding spectrum for exposures of (a) 0.9 and (b) 1.8 L of 2-butanol at 80 K.

background CO at higher exposures. The intense feature above 400 K is assigned to CO desorption due to 2-butanol decomposition, due mainly to CO formed by dissociation of 2-butoxide. At the lowest 2-butanol exposure (0.1 L), CO desorbs at ~490 K. This decreases to ~475 K at an exposure of 0.2 L and remains constant at ~460 K at 2-butanol exposures of 0.4 L and above. Fig. 8b plots the high-temperature CO yield as a function of 2-butanol exposure.

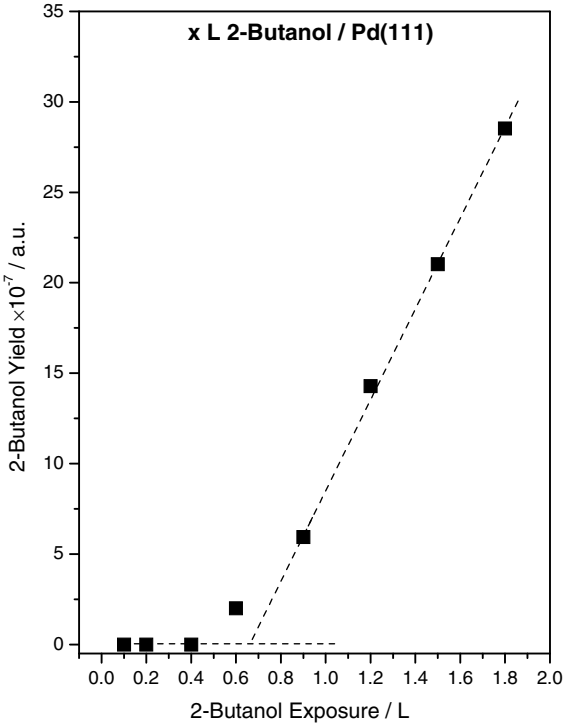

Fig. 6. Plot of molecular 2-butanol yield from temperature-programmed desorption experiments as a function of 2-butanol exposure at 80 K.

Similar to data shown in Fig. 7b, CO yield reaches the maximum at an exposure of 0.6 L. Note that at 2-butanol exposures of 1.5 and 1.8 L, there is a slight decrease in the CO yield. Presumably this is because the extent of dissociation decreases on a crowded surface.

5. Discussion

It has been demonstrated previously using reflection-absorption infrared spectroscopy that 2-butoxide forms on clean Pd(1 1 1) following exposure to 2-butanol at 100 K. The structure of 2-butoxide, calculated by DFT is in excellent agreement with structural determinations from the LEED data (Fig. 2) yielding a saturation 2-butoxide coverage of ~0.25–0.3 ML. The resulting structure is depicted in Fig. 1 and shows that the oxygen of the 2-butoxide species is bonded at the three-fold hollow site with the C–O bond perpendicular to the surface. The 2-butyl group is in a trans conformation and lies almost parallel to the (1 1 1) surface. RAIRS data also reveals that this 2-butoxide species forms 2-butanone via a β-hydride elimination reaction. This chemistry is relevant to the oxidation catalysis in which oxygen reacts with alcohols on gold-palladium alloys to form ketones implying that the clean single crystal surface can reproduce the chemistry occurring under catalytic conditions [27]. It is evident, however, that adsorption on clean palladium results in complete thermal decomposition of a portion of the adsorbed 2-butoxide to finally evolve hydrogen and carbon monoxide (Figs. 7 and 8). Presumably alloying with gold will decrease the surface reactivity to inhibit this total decomposition pathway. This effect is indeed found for 2-butanol chemistry on Au/Pd(1 1 1) alloy surfaces [28].

The surface chemistry can be divided into to rather distinct regimes. Below a 2-butanol exposure of ~0.7 L, no 2-butanol desorbs from the surface, while over the exposure range between 0 and ~0.7 L the yield of hydrogen (Fig. 7) and carbon dioxide (Fig. 8) increase. Assuming a relatively constant 2-butanol sticking coefficient, a saturation coverage of ~0.25 (Fig. 2) the coverage at an

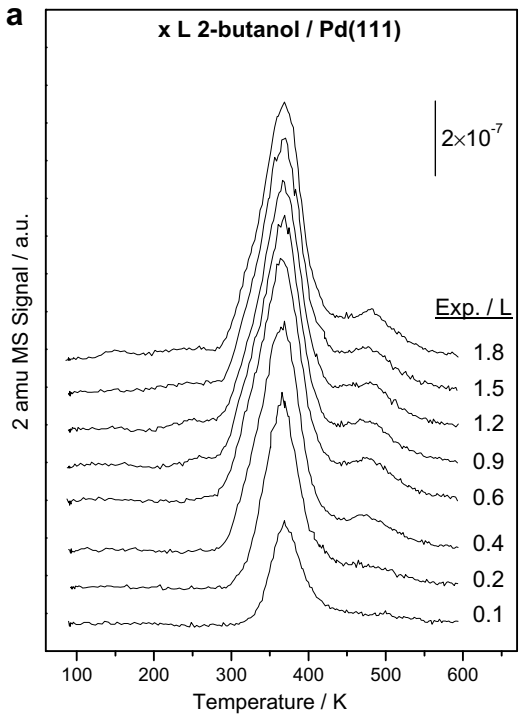

Fig. 7. (a) Temperature-programmed desorption data monitoring 2 amu (hydrogen) following adsorption of 2-butanol on clean Pd(1 1 1) at 80 K at a heating rate of 6.5 K/s as a function of 2-butanol exposure, where exposures are marked adjacent to the corresponding spectrum. (b) displays the total hydrogen yield, measured from the TPD spectra displayed in (a), as a function of 2-butanol exposures.

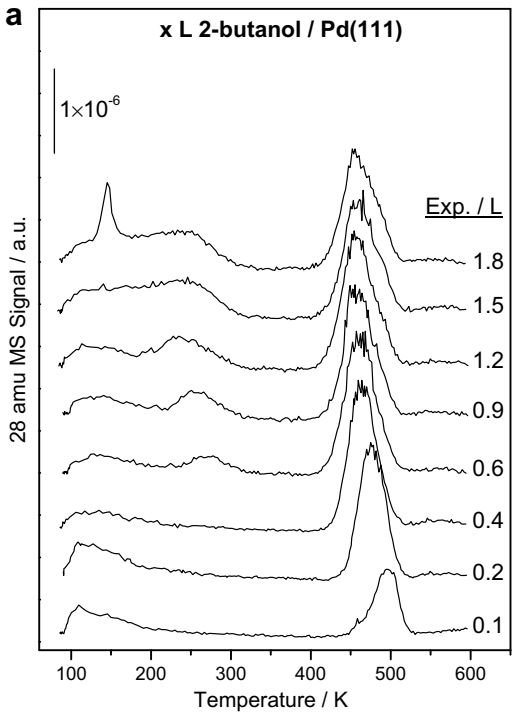

Fig. 8. (a) Temperature-programmed desorption data monitoring 28 amu (carbon monoxide) following adsorption of 2-butanol on clean Pd(1 1 1) at 80 K at a heating rate of 6.5 K/s as a function of 2-butanol exposure, where exposures are marked adjacent to the corresponding spectrum. (b) displays the total carbon monoxide yield, measured from the TPD spectra displayed in (a), as a function of 2-butanol exposures.

exposure of ~0.7 L is ~0.11. A structure with this 2-butoxide coverage is depicted schematically in Fig. 1 indicating that the 2-butoxide species are rather isolated at this coverage. Addition of further 2-butanol will lead to a more closely packed surface with 2-butoxide species adsorbed adjacent to each other. At this point, both 2-butanol (Fig. 3) and 2-butanone (Fig. 4) desorb from the surface where the yield of 2-butanol increases essentially linearly with 2-butanol exposure (Fig. 6). The 2-butanol desorbs between ~285 K and ~235 K depending on coverage (Fig. 3). Previous RAIRS results indicate the formation of 2-butoxide at ~200 K so that the 2-butanol formation detected in TPD likely arises due to the

rehydrogenation of adsorbed 2-butoxide species. The decrease in peak temperature with increasing coverage could be indicative of second-order desorption kinetics due to a surface reaction between adsorbed hydrogen and 2-butoxide species, or repulsive lateral interactions between adsorbates. At low exposures (~0.9 L), 2-butanone desorbs at approximately the same temperature as 2-butanol (Fig. 4b), but at higher coverages desorbs at lower temperatures. Since β-hydride elimination is a first-order process, the decrease in peak desorption temperature in this case is clearly due to interactions with neighboring (2-butoxide) species. Since crowding of the surface will likely inhibit dehydrogenation reactions by limiting access of the hydrogen to the surface, such a decrease in desorption temperature with increasing coverage implies that the activation energy for β-hydride elimination is lowered by interaction with neighboring species. Thus, at low coverages, when there are very few adjacent 2-butoxide species, there is sufficient space for the 2-butoxide to completely dehydrogenate. As neighboring 2-butoxide sites become occupied, total decomposition is inhibited and β-hydride elimination occurs with a relatively high activation energy. This can be estimated using the Redhead equation assuming that 2-butanone desorption in Fig. 4b reflects the β-hydride elimination kinetics as ~62 kJ/mol (taking a peak temperature of ~250 K and assuming a pre-exponential factor of 1×10^{13} s^{-1} [29]). As the coverage increases to saturation, the peak shifts to ~200 K yielding an activation energy of ~49 kJ/mol, due to lateral interactions.

6. Conclusion

2-butoxide formed on a Pd(1 1 1) surface following the adsorption of 2-butanol adsorb with the oxygen atom located in the three-fold hollow sites with the C–O bond almost perpendicular to the surface with the 2-butyl group in the trans configuration. For 2-butoxide coverages less than ~0.11, adsorbed 2-butoxide completely thermally decomposes. It is proposed that, at such low coverages, the adsorbed 2-butoxide species are sufficiently isolated to allow them to decompose. At higher coverages, 2-butoxide either hydrogenates to reform 2-butanol or undergoes a β-hydride elimination reaction to form 2-butanone. It is suggested that 2-butoxide thermal decomposition is inhibited at coverages above ~0.11 due to surface crowding.

Acknowledgments

We gratefully acknowledge support of this work by the US Department of Energy, Division of Chemical Sciences and Division of Materials Sciences and Engineering, Office of Basic Energy Sciences, under Grant numbers DE-FG02-00ER15091 and DE-FG02-84ER-45076, respectively.

References

[1] D. Stacchiola, L. Burkholder, W.T. Tysoe, J. Am. Chem. Soc. 124 (2002) 8984.
[2] D. Stacchiola, L. Burkholder, T. Zheng, M. Weinert, W.T. Tysoe, J. Phys. Chem. B 109 (2005) 851.
[3] F. Gao, Y. Wang, L. Burkholder, W.T. Tysoe, J. Am. Chem. Soc. 129 (2007) 15240.
[4] F. Gao, Y. Wang, W.T. Tysoe, J. Phys. Chem. C. 112 (2008) 6145.
[5] J.L. Davis, M.A. Barteau, Surf. Sci. 197 (1988) 123.
[6] J.L. Davis, M.A. Barteau, Surf. Sci. 235 (1988) 235.
[7] D.K. Saldin, V.L. Shneerson, J. Phys.: Condens. Matter, in press.
[8] J.B. Pendry, Low Energy Electron Diffraction, Academic Press, London, 1974.
[9] M. Kaltchev, W.T. Tysoe, J. Catal. 196 (2000) 40.
[10] H.C. Poon, X.F. Hua, S.E. Chamberlin, D.K. Saldin, C.J. Hirschmugl, Surf. Sci. 600 (2006) 2505.
[11] M.A. Van Hove, R. Lin, G.A. Somorjai, Phys. Rev. Lett. 51 (1983) 778.
[12] D.K. Saldin, J.B. Pendry, M.A. Van Hove, G.A. Somorjai, Phys. Rev. B 31 (1985) 1216.
[13] N. Bickel, K. Heinz, Surf. Sci. 163 (1985) 435.
[14] T. Zheng, W.T. Tysoe, H.C. Poon, D.K. Saldin, Surf. Sci. 543 (2003) 19.
[15] H.C. Poon, M. Weinert, D.K. Saldin, D. Stacchiola, T. Zheng, W.T. Tysoe, Phys. Rev. B. 69 (2004) 035401.
[16] T. Zheng, D. Stacchiola, H.C. Poon, D.K. Saldin, W.T. Tysoe, Surf. Sci. 564 (2004) 71.
[17] T. Zheng, D. Stacchiola, D.K. Saldin, J. James, D.S. Sholl, W.T. Tysoe, Surf. Sci. 574 (2005) 166.
[18] J. James, D.K. Saldin, T. Zheng, W.T. Tysoe, D.S. Sholl, Catal. Today 105 (2005) 74.
[19] G. Kresse, H. Hafner, Phys. Rev. B 47 (1993) 558.
[20] F. Starrost, E.A. Carter, Surf. Sci. 500 (2002) 323.
[21] P.J. Feibelman, B. Hammer, J.K. Nørskov, F. Wagner, M. Scheffler, R. Stumpf, R. Watwe, J. Dumesic, J. Phys. Chem. B 105 (2001) 4018.
[22] J.P. Perdew, J.A. Chevary, S.H. Vosko, K.A. Jackson, M.R. Pederson, D.J. Singh, C. Fiolhais, Phys. Rev. B 46 (1992) 6671.
[23] J.H. Monkhorst, J.D. Pack, Phys. Rev. B 13 (1976) 5188.
[24] D.R. Lide, E.H.I.R. Frederikse (Eds.), CRC Handbook of Chemistry and Physics, 83rd ed., CRC Press, New York, 2002.
[25] J. Neugebauer, M. Scheffler, Phys. Rev. B 46 (1992) 16067.
[26] J.B. Pendry, J. Phys. C 13 (1980) 937.
[27] D.I. Enache, J.K. Edwards, P. Landon, B. Solsona-Espriu, A.F. Carley, A.A. Herzing, M. Watanabe, C.J. Kiely, D.W. Knight, G.J. Hutchings, Science 311 (2006) 362.
[28] F. Gao, Y. Wang, Z. Li, O. Furlong, W.T. Tysoe, J. Phys. Chem. C 112 (2008) 3362.
[29] P.A. Redhead, Vacuum 12 (1962) 203.